PHYSICAL REVIEW B VOLUME 14, NUMBER 4 15 AUGUST 1976

Realistic tight-binding model for chemisorption: H on Si and Ge (111)

K. C. Pandey*
Bell Laboratories, Murray Hill, New Jersey 07974
(Received 6 January 1976)

A realistic tight-binding model for chemisorption on semiconductor surfaces is presented. The model is quantitatively accurate, computationally very simple, free from adjustable parameters, and can be applied to a wide variety of problems. The basic assumption underlying the model, which is based on the Hückel approximation, is that the local bond (i.e., the chemisorption bond) at the surface is similar to the corresponding bond in an appropriately chosen molecule. While the Hamiltonian matrix elements between substrate atomic orbitals are determined from the well-known bulk energy bands, the matrix elements between chemisorbate and substrate orbitals are obtained from molecular energy levels. The matrix elements thus obtained show reasonable chemical trends. The validity of the above procedure for the determination of the matrix elements is demonstrated by the good agreement of the theoretical spectra with experiment obtained without further adjustment of parameters. The sensitivity of the spectra to changes in the parameters is described in detail. The surface-energy bands and local density of states have been calculated for the chemisorption of atomic hydrogen on the (111) surfaces of Si and Ge. The apparent photoelectron density-of-states spectrum has been calculated taking into account the escape probability, the secondary electrons, and the variation of the oscillator strength near the surface (local oscillator strength). The calculated spectra are in excellent agreement with experiment.

I. INTRODUCTION

The ultraviolet-photoemission spectra (UPS) of cleaved Si and Ge (111)2×1 surfaces undergo dramatic changes on exposure to atomic hydrogen.[1-3] The large peak just near the valence-band maximum (VBM) which is associated with the broken or dangling bond at the surface[4-8] disappears while a new peak appears at about 5.0 eV below VBM. Various features in the spectra that have been associated[9-13] with the strengthening of the back bonds at the surface (due to the relaxation of the surface atoms) also disappear, but the peak at about 7.5 eV below VBM (associated with the bulk bands) is enhanced. Further, the low-energy-electron-diffraction pattern changes to the primitive 1×1 structure.

The most important factor governing the electronic structure of cleaved surfaces is the presence of unsaturated dangling bonds which give rise to the relaxation and Jahn-Teller distortion of the surface atoms leading to the 2×1 reconstruction.[11,12] Qualitative understanding of the effects of atomic-hydrogen chemisorption can be obtained by noting that the dangling bonds, being chemically most active, will form strong Si–H bonds similar to those in SiH_4 molecule. Because of the saturation of the dangling bonds, the surface atoms of the semi-infinite Si lattice do not relax or undergo Jahn-Teller distortion (leading to 1×1 structure). The appearance of new peaks in the photoemission spectra can be associated with the H–Si bond.

In this paper we present a *realistic* tight-binding (TB) model calculation[11] of the surface energy bands of Si and Ge (111)1×1 covered with a monolayer of hydrogen. Detailed interpretation of the photoemission spectra is provided in terms of the local density of states (LDS).

An essential ingredient to the TB calculations is the knowledge of the Hamiltonian matrix elements between various atomic orbitals involved. However, a first-principles calculation of these matrix elements is very tedious and in this paper we take a semiempirical tight-binding (SETB) approach.[10-13] Basic to this approach is the assumption that the two-center matrix elements between the orthogonalized orbitals (Hückel approximation) are transferable from one system to the other provided the bond lengths remain unchanged. Further, these matrix elements are obtained by fitting to the known electronic energy levels of a molecule or solid consisting of the bonds in question.

In spite of the bad reputation the TB method has had in the past, for energy bands of nonionic solids, we want to emphasize that the present calculations are quantitatively accurate and that in general the TB method is quite capable of giving quantitatively accurate results for valence states of covalent crystals in the bulk as well as at surface. In earlier publications,[10-13] TB calculations for bulk and various clean surfaces, e.g.,[10,11,13] Si and Ge (111)1×1 and[11] (100)1×1 (both the ideal and relaxed) as well as[12] Si(111)2×1 have been presented. These calculations have, for the first time with the TB method, been able to provide an adequate explanation[10-13] for the various surface-sensitive features observed in UPS,[7,8] electron

energy loss[6] and ion-neutralization spectroscopic[14] experiments. Further, for all cases for which first-principles self-consistent[9] calculations have been carried out, the two calculations,[11,13] are in excellent quantitative agreement, showing the validity of the TB model for valence states.

This paper is organized as follows: In Sec. II we discuss the chemisorption model and the determination of the Hamiltonian matrix elements between the chemisorbate and substrate atomic orbitals. A discussion of the chemical trends of the parameters thus obtained is provided. Section III deals with the calculation of surface energy bands and LDS. The nature of the surface states and resonances that give rise to structures in the LDS are discussed in terms of the atomic orbitals. In Sec. IV, the apparent photoemission density of states has been calculated, taking into account escape probabilities for electrons and secondary electron emission. Matrix-element effects (optical oscillator strengths) are also included in an approximate way. Theoretical results for Ge and Si (111), both clean and hydrogen covered, are compared to experimental photoemission data in Sec. V. The agreement with experiment and theory is found to be excellent. Section VI discussed the validity of the present model, its practical usefulness in other problems and possible extensions. Molecular energy levels of SiH_4 and GeH_4 are discussed in Appendix A. A brief discussion of the secondary electron distribution is provided in Appendix B.

II. THE CHEMISORPTION MODEL: DETERMINATION OF PARAMETERS

The most important ingredient in the SETB calculations is knowledge of the Hamiltonian matrix elements (parameters) between the valence orbitals of the constituent atoms. These orbitals are assumed to be orthogonalized (Hückel approximation). In principle, these parameters can be obtained from a first-principles calculation, but in practice, it is more convenient to use a semiempirical approach. In SETB method, these parameters are obtained from the electronic states of the system which are generally known either from experiments or from *ab initio* calculations.

A detailed calculation of the bulk energy bands of Si and Ge using the SETB method has been given elsewhere.[13] The seven parameters in these calculations have been obtained after an extensive search in parameter space using a least-squares fit to the well-known energy bands[15,16] at a large number of $\vec{k}$ points in the Brillouin zone. Since the TB method, based only on the valence orbitals (minimal basis set) is not suited for the representation of higher conduction bands, all but the lowest two conduction bands have been ignored in the fitting procedure. The latter is included only with half the statistical weight. It should be noted that in the present calculations we are mainly concerned with the valence states.

TABLE I. Tight-binding interaction parameters for Si and Ge (in eV). The subscripts 1 and 2 refer to the first and second nearest neighbors. Note the systematic variation of the parameters.

Parameters	Si	Ge
$E_p - E_s$	4.39	6.44
$(ss\sigma)_1$	−2.08	−1.69
$(sp\sigma)_1$	−2.12	−2.03
$(pp\sigma)_1$	−2.32	−2.55
$(pp\pi)_1$	−0.52	−0.67
$(pp\sigma)_2$	−0.58	−0.41
$(pp\pi)_2$	−0.10	−0.08

The parameters[13] for Si and Ge are listed for the reader's convenience in Table I and the energy bands of Si are shown in Fig. 1, where they are compared with experiment and pseudopotential calculation.[15] In contrast to many other TB calculations,[17] the present valence energy bands

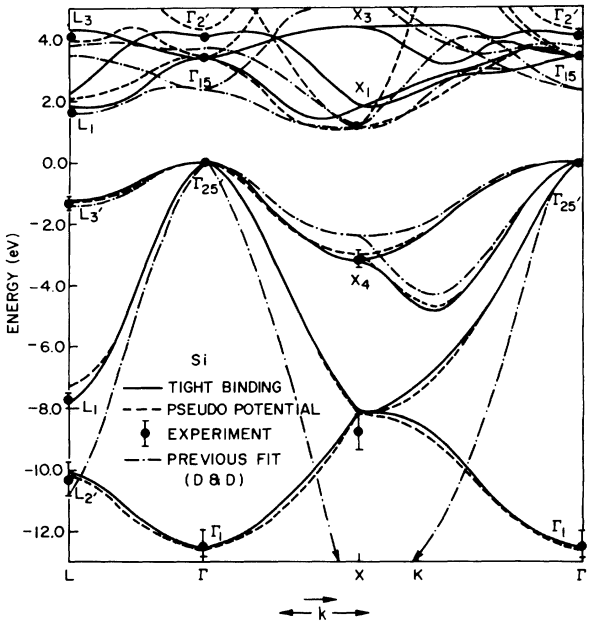

FIG. 1. Present tight-binding fit to the energy bands of Si using a seven first- and second-neighbor paramaters is compared with pseudopotential energy bands (Ref. 15) and an earlier thirteen-parameter first- and second-neighbor fit (Ref. 17). The latter energy bands, in spite of the abundance of adjustable parameters in the model, are in serious disagreement with experiments.

are in excellent quantitative agreement (within ~2%) with experiment. Equally good results are obtained for Ge as well.[13,16] The least-squares error associated with the overall fit is of order 0.3 eV, and the uncertainties in the larger parameters ($E_p - E_s$ and the first-neighbor interaction energies) are of this order.

Having determined the interaction parameters for the bulk, the electronic states of the substrate are completely specified, since deep inside the crystal, the atomic arrangement, crystal potential, etc., are expected to be the same as in bulk. However, the situation at the surface is much more complicated. Fortunately, a highly plausible model based on chemical ideas can be constructed in the present case. The ideal (111) surface of Si and Ge is characterized by a single broken (dangling) bond that points perpendicular to the surface. When the surface is covered with a monolayer of atomic hydrogen, these chemically active bonds can be saturated by forming strong H–Si (Ge) bonds. The disappearance of 2×1 superstructure (in low-energy-electron diffraction) from cleaved surfaces on chemisorption supports such bond formation. Further, the remarkable constancy of bond lengths in various molecules suggests that the H–Si (Ge) bond length at the surface is the same as the H–Si (Ge) bond length in SiH_4 (GeH_4). Thus the hydrogen monolayer is assumed to be separated from the substrate by 1.48 and 1.53 Å for Si and Ge, respectively. Further support for the above argument is obtained from the experimental studies[18] of the vibrational frequency (bond stretching mode) associated with the Si–H bond in SiH_4 and at the surface. The two frequencies are in good agreement with each other. It should be noted that above arguments are expected to hold for the chemisorption of other monovalent atoms (e.g., Cl) as well.

In order to study chemisorption, the only matrix elements that are as yet unspecified are those between H and Si (Ge) orbitals, the Si–Si (Ge–Ge) parameters having been determined once and for all from the bulk energy bands as discussed earlier. In the spirit of SETB method, we determine these matrix elements from the molecular energy levels of SiH_4 and GeH_4 which can be taken as a more precise statement of the present chemisorption model.

The valence energy levels of SiH_4 and GeH_4 are known from x-ray photoemission experiments.[19] Unoccupied levels for these molecules are also available from theoretical calculations.[20] These molecular levels are listed in Table II. Theoretical expressions for the molecular energy levels are very easily obtained using the symmetry of the molecule and are given in Appendix A. From these molecular data, the most important of the matrix elements E_H (the diagonal element for the hydrogen orbital), and nearest-neighbor H–Si and H–Ge interaction parameters are uniquely determined. These parameters are listed in Table III. The H–Si matrix elements can be checked against the molecular energy levels of Si_2H_6 for which UPS results[21] are also available. Theoretical results for the molecular energy levels, which are also listed in Table II, are in good agreement with experiment.

To facilitate comparison of our Hückel parameters with those used in semiempirical molecular orbital calculations, we have referenced our diagonal energies to $E=0$ in vacuum. Most semi-

TABLE II. Molecular energy levels (in eV, relative to vacuum) of SiH_4, Si_2H_6, and GeH_4. The positions of the unoccupied levels are obtained from the first principles calculations (Ref. 20). Molecular orbitals are labeled by their standard symmetry notation (see e.g., Ref. 21).

	Experiment	Theory
SiH_4		
a_1^-	−4.1 [a]	−4.01
t_2^-	−5.4 [a]	−5.33
t_2^+	−12.7 [b]	−12.62
a_1^+	−18.2 [c]	−18.33
Si_2H_6		
a_g	−10.7 [c]	−10.79
e_g	−12.1 [c]	−12.50
e_u	−13.3 [c]	−12.76
a_u	−17.3 [c]	−16.91
GeH_4		
a_1^-	−4.9 [a]	−5.17
t_2^-	−5.2 [a]	−5.28
t_2^+	−12.3 [b]	−11.96
a_1^+	−18.5 [b]	−18.50

[a] See Ref. 20.
[b] See Ref. 19.
[c] See Ref. 21.

TABLE III. Matrix elements (eV) between hydrogen orbitals and the orbitals of Si and Ge. The zero of the energy is taken at the top of the bulk valence band.

	Si	Ge
E_H	−3.38	−3.81
$ss\sigma$	−3.57	−3.30
$sp\sigma$	−2.76	−2.15

empirical molecular schemes introduce atomic energies either through one-electron ionization energies E_I (extended Hückel method)[22] or through the average of E_I and the electron affinity E_A (Hückel or Pople methods).[23] No rigorous demonstration of the validity of either definition can be given, as both definitions depend on a somewhat arbitrary choice of basis functions. The Hückel-Pople definition is, of course, based on Mulliken's definition of atomic electronegativities.[24]

In the present context we are constrained to use a Hückel approach by the success and simplicity of this method in fitting the bulk energy bands of Si and Ge. Thus we would expect to find that our atomic energy parameters should lie closer to $\frac{1}{2}(E_I+E_A)$ than to E_I. However, from our present point of view there is no need to introduce the atomic energy levels of *isolated* atoms into the calculation. Rather we prefer to derive all parameters, including the atomic energy levels themselves, from the measured spectra of atoms in bonded states. (In the present case this means the energy levels of bulk Si and Ge and SiH_4 and GeH_4.) This corresponds to defining the Hückel atomic energy parameters in the spirit of Pauling's electronegativity parameters (which represent "the power of atoms in bonded states to attract electrons to themselves").[25]

In Table IV we compare our atomic energy parameters for SiH_4 and GeH_4 with those given by[23] $\frac{1}{2}(E_I+E_A)$. For SiH_4 we use the Si parameters from bulk Si, for GeH_4 from bulk Ge. The differences between E_H and $E_{s,p}$ for Si (Ge) are determined by fitting the energy differences of SiH_4 (GeH_4) molecules, instead of absolute energy levels. (This minimizes corrections due to breakdown of the Koopmanns theorem.) Thus we introduce I_p(Si) and I_p(Ge), the ionization potentials of the crystals (both taken to be 4.8 eV) into referencing E_H and we obtain two values of E_H, which are to be compared with the single value of E_H obtained from the atomic prescription.

The most important conclusions which can be drawn from the data shown in Table IV are first, that E_H (and the other parameters as well) lie closer to $\frac{1}{2}(E_I+E_A)$ than to E_I (as expected), but that the differences between our parameters and the atomic parameters are significant. This conclusion follows from noticing that the apparent difference in E_H in SiH_4 and GeH_4 is 0.4 eV (which is of the order of the uncertainties in the photoemission energies determined experimentally, see Table II), while the shift from the atomic values is about 1 eV. The shifts in E_s(Si) and E_s(Ge) from the atomic values are opposite in sign from those of E_H and of nearly the same magnitude. The shifts of E_p(Si) and E_p(Ge) are very small. While these differences are considered small for most semiempirical molecular-orbital calculations, they are significant to us because perceptibly poorer results are obtained in fitting to observed spectra (bulk, molecular, or chemisorbed) when the atomic energies are shifted by as much as 1 eV. (We illustrate this point in Sec. VI for the particular case of chemisorption discussed here.)

As mentioned earlier, the H–Si (Ge) matrix elements are determined from the molecular energy differences of SiH_4 (GeH_4). The absolute position of the atomic energy levels of Si (Ge) in the crystalline form can be obtained from the ionization potential. The Si (Ge) atomic energies in the crystal thus obtained lie about 1.7 eV higher than the corresponding energies obtained from molecular data (by shifting the atomic energies so that the calculated levels are in agreement with experiment). Such a shift is significant and not unexpected. The molecular energy levels listed in Table II are in fact the ionization potentials[26] of the various molecular levels. Due to the large relaxation effect in molecules, the ionization potential is larger than that derived from the one-electron levels of the ground state. This apparent downward shift of one-electron levels is very nearly the same for all the levels. Due to the extended nature of states, relaxation effects are not important in solids.

TABLE IV. Atomic energies (diagonal matrix elements) of hydrogen and s and p orbitals of Si and Ge obtained in the present calculation are compared with the corresponding atomic energies used in Pople's method (Ref. 23).

	SiH_4		GeH_4	
	Present	Atomic	Present	Atomic
E_H	−8.18	−7.18	−8.61	−7.18
$E_s(x)$	−9.00	−10.03	−10.58	−11.43
$E_p(x)$	−4.61	−4.13	−4.14	−4.08

III. SURFACE CALCULATIONS

The calculations of the surface energy bands and local density of states (LDS) for hydrogen chemisorption are very similar to those for clean surfaces which are discussed in detail elsewhere.[11,13] In the present case a slab of 28 Si (Ge) atomic layers bounded on both sides by a hydrogen layer was used. The small interaction (<0.01 eV) between the two surface states (localized on opposite surfaces) and the close agreement (within ~3%) of the LDS in the center of the slab with the bulk density of states shows that for all practical purposes, the slab is of infinite thickness. The

effect of finite thickness on the LDS at the hydrogen layer is discussed in Sec. VI.

The most notable feature of the electronic structure is the appearance of a surface band corresponding to the strong Si–H bond. There are true surface states only near the surface-Brillouin-zone (SBZ) boundary (Fig. 2). Over a larger region of $\vec{k}_{\parallel}$ space near the SBZ center, surface resonances at ~7.0 eV (below VBM) dominate the energy band spectrum. In addition, near K point (Γ, J, and K are the points in the hexagonal SBZ that are located at the zone center, edge center, and corner respectively), there are two true surface states split off from the bulk bands due to the strong perturbation at the surface. The energies of the surface states at J and K for Si and Ge are listed in Table V.

The LDS at the hydrogen atoms $[\rho_1(E)]$ and three successive Si layers $[\rho_i(E), i=2,3,4]$ are shown in Fig. 3 where they are compared with the bulk density of states (dashed curves). These were

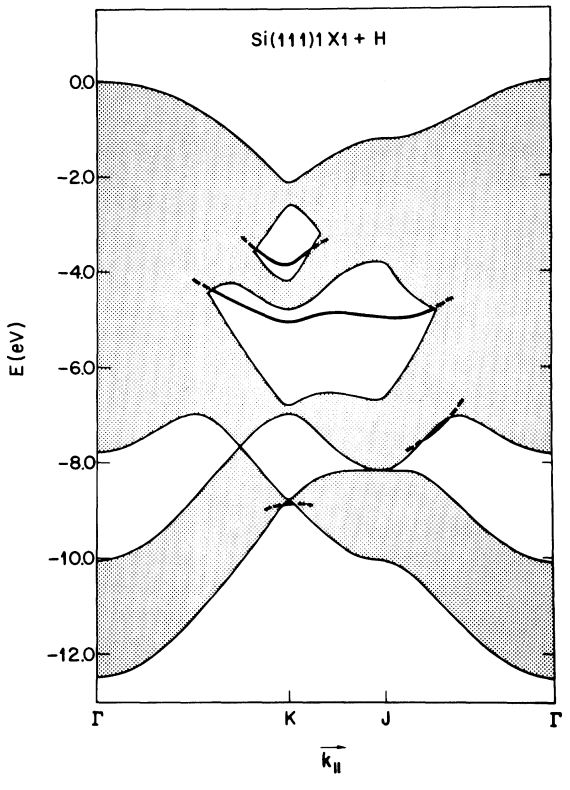

FIG. 2. Surface energy bands for hydrogen chemisorbed on Si(111)1×1. For a fixed surface wave vector $\vec{k}_{\parallel}$ true surface states (shown by heavy lines) exist only in the energy gap of the bulk bands obtained by varying $\vec{k}_{\perp}$. The region where no such gap exists is shown by the dotted area. The center of the surface Brillouin zone (a hexagon) is denoted by Γ. The edge center and corner are denoted by J and K respectively.

TABLE V. Surface state energies at J and K points in the two-dimensional Brillouin zone. There are no surface states at Γ point, one at J, and three at K (Fig. 2). The points Γ, J, and K refer to the center of the zone, center of the edge and corner, respectively.

$\vec{k}_{\parallel}$	Si	Ge
J	−4.94	−4.62
K	−3.88	−3.77
	−5.02	−4.70
	−8.83	−9.44

obtained by sampling a grid of 21 points $\vec{k}_{\parallel}$ in the irreducible section of the SBZ. The basic sample of 21 points was augmented by a factor of 100 by interpolation (using Fourier expansion). The total sample thus obtained was used to construct histograms for the density of states.

As expected, the LDS on the hydrogen layer $[\rho_1(E)]$ differs drastically from the bulk density of states (BDS). The most prominent feature of $\rho_1(E)$ is the large logarithmic peak at about −5.0 eV (below VBM). This peak arises from the saddle point (near J in the SBZ) in the true surface state energy band (Fig. 2). In view of the nature of the surface state band, this peak can be associated with the Si–H bond.

The peaks at −7.0 and −10.0 eV in $\rho_1(E)$ are due to surface resonances which are distributed throughout this energy region (Fig. 2). Consequently, the shape of the peaks and their positions are very similar to the corresponding peaks in the BDS. (It should be noted that the densities of

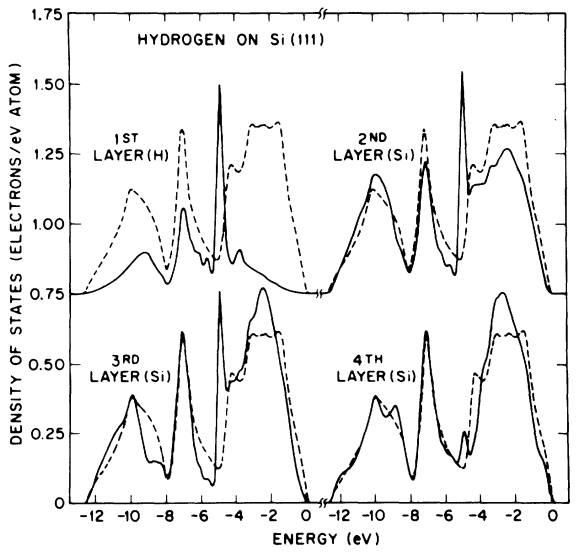

FIG. 3. Local density of states for the hydrogen and three successive layers of Si. The bulk density of states are shown by the dashed curves.

states shown in Fig. 3 are normalized according to the number of electrons/atom.) However, there are two main differences. First, the relative height of the peak at −7.0 eV compared to the one at −10.0 eV is larger in $\rho_1(E)$ than it is in the BDS, so that if $\rho_1(E)$ and BDS are normalized to the same value, the −7.0 eV peak in $\rho_1(E)$ is enhanced over BDS. This can be easily explained by noting that the states that contribute to the peak at −7.0 eV are closer in energy to the hydrogen 1*s* orbital, leading to stronger hybridization. The enhancement of this peak (over the bulk) is due to the increased strength of the Si–H bond relative to the Si–Si bond. Secondly, the peak in $\rho_1(E)$ due to the *s* band (at about −10.0 eV), lies at a higher energy compared to the corresponding peak in the BDS. This apparent shift is due to the contribution to $\rho_1(E)$ from the surface states and resonances (near K in the SBZ, Fig. 2) and can again be ascribed to the stronger Si–H bond.

Another interesting feature of $\rho_1(E)$ is that, apart from the small peak at about −3.5 eV which is due to the surface states near K (Fig. 2), $\rho_1(E)$ is very small in the energy region 0 to −4.0 eV. Looking at the BDS we find a large density of states (a total of about 2 electrons/atom) in this energy region and one expects a large $\rho_1(E)$ as well. However, the electrons in this region are mostly of π symmetry (with respect to $\vec{k}$). The most relevant wave vector for the surface is $\vec{k}_\perp$, so that the available Si states are mostly the $p\pi$ orbitals that lie in the surface plane and thus can not hybridize with the hydrogen σ orbital.

Chemisorption bond formation is clearly reflected in the local density of states $\rho_2(E)$ for the Si atoms at the surface (Fig. 3). The sharp peak at −5.0 eV [similar to the peak in $\rho_1(E)$] is due to the Si $p\sigma$ electrons taking part in bond formation. These electrons are derived from the higher-energy region (Fig. 3) thus lowering the energy. Nearly equal heights of the peaks in $\rho_1(E)$ and $\rho_2(E)$ are an indication of the nature of the surface state wave functions which consist of nearly equal amounts of hydrogen 1*s* and Si $3p_{111}$ orbitals.

Even though the second-layer Si atoms are not directly bonded to the hydrogen atoms, surprisingly, their local density of states, $\rho_3(E)$ (Fig. 3), also shows a sharp peak at −5.0 eV [similar to those in $\rho_1(E)$ and $\rho_2(E)$]. Obviously, this peak also arises from the saddle point in the surface state energy band (Fig. 2), and is due to the particular nature of the wave function. As opposed to molecules, the surface state wave functions inside the crystal are a linear combination of the bulk states for a given $\vec{k}_\parallel$. Since the density of states is generally dominated by critical points $\vec{k}_\parallel^c$, the LDS reflect their symmetry and the nature of their wave function as well. In the present case, as a result of the above constraint, the surface state wave function is such that the p_{111} orbital of the Si atom at the surface occurs together with a $p_{\bar{1}11}$ orbital on the second atom with almost equal amplitude. This effect can be described as a "solid state effect." For the clean Si(111)1×1 surface,[13] we have observed similar effects in the dangling bond density of states where the LDS at the fourth layer (in addition to the first layer) is unexpectedly large. These effects are obviously absent in the cluster of "surface molecule"[27] models of chemisorption, casting some doubt on their overall applicability.

As we move further into the crystal, the LDS approaches the BDS due to the exponential decay of the surface state wave functions. For example, the LDS of the third Si atom $\rho_4(E)$ (Fig. 3), shows only a small peak at −5.0 eV arising from the surface states. The small features in the LDS of this and other layers are due to surface resonances which show complicated oscillatory behavior depending on the details of the energy bands. However, a common feature of the LDS on Si layers, near the surface is the narrowing of the density of states peak at −2.0 eV (due to the π electrons). Such a narrowing is a general occurrence on free surfaces and can be qualitatively understood in simple TB models.[28]

IV. APPARENT PHOTOELECTRON DENSITY OF STATES

The observed energy distribution $N(E)$ of photoexcited electrons consists of two parts,

$$N(E) = N_p(E) + N_s(E) , \tag{1}$$

where $N_p(E)$ is the energy distribution of primary electrons and $N_s(E)$ is the energy distribution of secondary electrons. As described in detail in Appendix B, one can calculate $N_s(E)$ using Kane's methods[29] for treating Auger scattering and using the density of valence and conduction band states of bulk Si. In the interest of simplicity, alternatively one could assume that $N_s(E)$ was described by some smooth curve with a simple algebraic form as has been done in the past.[7] However, such a procedure is arbitrary. We therefore calculated $N_s(E)$ following Kane's prescription and adjusted its magnitude to agree with $N(E)$ at low energies, where $N_p(E) = 0$. This procedure was also used in calculations of bulk photoemission spectra,[4,30] and the results were quite satisfactory.

To obtain $N_p(E)$ we have assumed that the oscillator strength for bulk excitations is approximately independent of energy over most of the valence bands. The oscillator strength of the

lowest (s-like) valence band is very small for photon energies below 23 eV, and becomes comparable to that of the other valence bands at higher energies, as observed in photoemission experiments on Ge with synchrotron radiation.[4,30] Between 16 and 21 eV, the bulk oscillator strength of the second lowest valence band also increases. These changes can be explained by assuming that the lowest conduction bands correspond to antibonding combinations of p atomic orbitals, and that the next group of conduction bands has predominantly bonding d character. Above these bands, and starting about 25 eV above the 2-eV-wise s-valence band, lie most of the antibonding s states.

The data we have analyzed are based on photon energies of 21.1 and 16.8 eV. Our assumption of constant oscillator strengths is better justified for the higher photon energy, but even at $\hbar\omega = 21.1$ eV the oscillator strength of the lowest valence band is small. We have therefore suppressed this contribution to $N_p(E)$ in the corresponding spectral region.

In order to illustrate this idea, in Fig. 4 we present the s and p partial density of states in the bulk and at the first Si atomic layer. As expected, the largest s contribution to the density of states arises at lower energies (~ -10.0 eV) and this contribution decreases rapidly as the energy increases. [It should be noted (Fig. 4) that there is substantial s contribution to the large peak in $\rho_2(E)$ at -5.0 eV.] As discussed above, due to the suppression of the s oscillator strengths for $\hbar\omega \approx 20.0$ eV, the primary electron spectrum $N_p(E)$ will resemble the p part of the density of states.

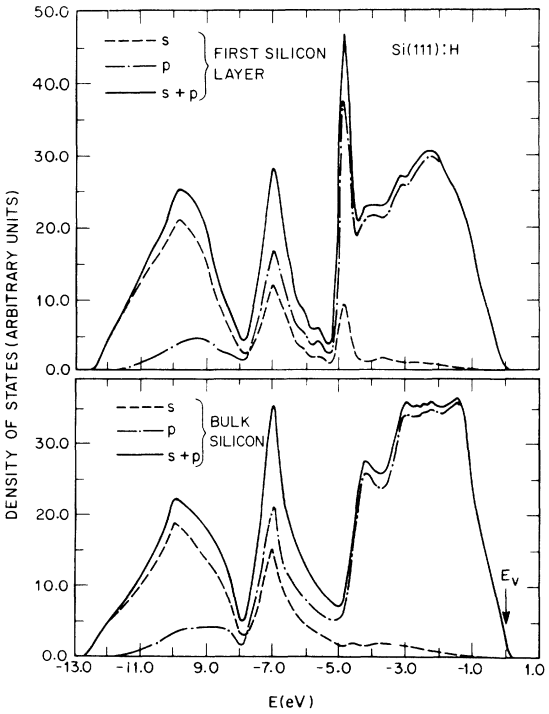

FIG. 4. Partial density of states for bulk Si and the first layer Si in Si(111):H.

Because of the small escape depth ($L \approx 5$ Å at $\hbar\omega = 21.2$ eV) of photoexcited electrons, different atomic layers do not contribute equally to the photoemission density of states for the primaries, which can be written with weighting parameters α_s and α_p as

$$N_p(E) = \sum_l r_l a_l [\alpha_p n_l^p(E) + \alpha_s n_l^s(E)] , \tag{2}$$

where the sum is over the different atomic layers (l), $n_l^p(E)$, and $n_l^s(E)$ are the p and s partial local density of states,[31] and a_l is an escape factor which can be approximated by

$$a_l \approx e^{-Z_l/L} , \tag{3}$$

Z_l being the distance of the lth layer from the surface. In Eq. (2) we have included a factor r_l (local oscillator strength) to account for the variation of the average (energy and momentum independent) oscillator strengths for photoexcitation. We have shown earlier[32] that the average oscillator strength depends very strongly on the nature of bonding. The bonding is most drastically altered at the surface, while in the crystal it remains almost identical to the bulk. Thus we can assume that in terms of surface and bulk oscillator strengths,

$$r_1 = r_S ,$$

$$r_l = r_B \quad (l > 1) ,$$

and Eq. (2) can be written

$$N_p(E) = r_S n_1^p(E) + r_B \sum_{l>1} a_l n_l^p(E) , \tag{4}$$

where we have put $\alpha_p = 1$ and $\alpha_s = 0$ as discussed earlier.

A detailed discussion of the dependence of r_S on the surface condition has been given elsewhere.[32] Here it suffices to mention that in general $r_S/r_B \gtrless 1$ depending on whether the bond at the surface is stronger or weaker than the bulk bonds. We have estimated[32] that $r_S/r_B \approx 5$ for hydrogen chemisorption on the (111) surfaces of Si and Ge. For clean Si and Ge (111) surfaces $r_S/r_B \approx 0.04$ for the dangling bond states, while for the back bonding states $r_S/r_B \gtrsim 1$. For convenience we take $r_S/r_B = 1$ for the back bonding states of clean (111) surfaces.

After the theoretical value of $N_p(E)$ has been computed from Eq. (4) in the form of a histogram

TABLE VI. Parameters used in the theoretical calculation of the photoemission spectra of clean and hydrogenated Si and Ge (111).

	$\hbar\omega$	α_s	α_p	L(Å)	Γ(eV)	E_{VB}	r_s
Si(111)7×7	16.8; 21.2	0	1	10; 5	0.6	4.8	0.05
Si(111):H	16.8; 21.2	0	1	10; 5	0.3	5.0	10.0
Ge(111):H	21.2	0	1	10	0.3	5.0	10.0

with energy intervals of 0.1 eV, it is combined with $N_s(E)$ to obtain $N(E)$. The theoretical expression for $N(E)$ so obtained is then convoluted with a Lorentzian broadening factor Γ (half-width). Three parameters [a scale factor for $N_s(E)$, Γ, and r_S] are then adjusted by a least-squares method to give the best fit to experiment (see Table VI). The adjustment of these parameters is unambiguous, if the mean-free path L in Eq. (3) is known. In fact, L is not known to better than a factor of two. However, the variations in $n_i(E)$ are such that for reasonable values of $L(\gtrsim 5$ Å), the best fit is obtained for $r_S L = \text{const}$. Moreover, no choice of L will give a satisfactory fit to the experimental data for Si(111):H with $r_S = r_B$. Though L varies with the energy of the excited electron, in the present calculations we have made the simplifying assumption that it depends only on the photon energy. Such an assumption seems reasonable since we are mainly interested in the electrons excited from a rather narrow energy region (around −10 eV). We have taken $L = 5$ and 10 Å for the photon energies $\hbar\omega = 21.2$ and 16.8 eV respectively. These are in accord with the available experimental data and lead to the values (Table VI) of r_S (from fitting to the UPS data) that are in good agreement with our estimates discussed above. The order-of-magnitude variation in r_S in going from clean to the hydrogenated surface clearly shows the strong dependence of the surface oscillator strengths on the nature of bonding at surface. These variations are adequately explained by our simple dispersion model.[32]

V. COMPARISON WITH EXPERIMENT

The theoretical results for the primary $[N_p(E)]$ and secondary $[N_s(E)]$ electron distributions at the photon energy of $\hbar\omega = 21.2$ eV are shown in Fig. 5 by dashed and dotted lines respectively. Similar results for the hydrogen chemisorbed Si(111) are shown in Fig. 6. Also shown in Figs. 5 and 6 are the UPS results of Sakurai and Hagstrum,[2] which are compared with $N(E)$.

The theoretical calculations presented in Fig. 5 are based on relaxed Si(111)1×1 surface. We have shown earlier[13] that most of the features in the UPS spectra of annealed Si(111) can be accounted for very satisfactorily by the simple relaxation model. The only region where such a model is unsatisfactory is near the top of the valence band where the annealed surface shows a very broad shoulder. This is expected since the annealed surface has a 7×7 reconstruction so that the dangling bond band is split in a complicated manner which given the experimental resolution would appear as broadening. This splitting is, of course, missing from the simple relaxation model. Based on the above argument we conclude that, in general, the features in the (111)1×1 theoretical spectrum should resemble those in the experimental data quite closely, and this is indeed seen to be the case in Fig. 5.

The agreement between theory and experiment shown in Fig. 5 is almost complete. The peak labeled A is broader in the experimental data than in the theory, and a shoulder D is barely evident in the data which is absent from the theory. On annealing,[2] considerable variation in the spectrum is observed at ~−6 eV and the peak A broadens

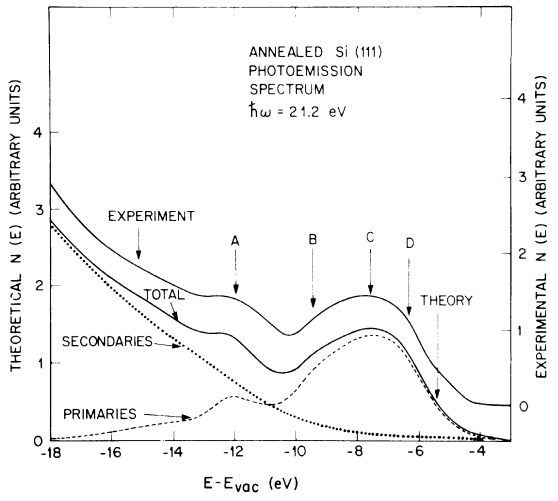

FIG. 5. Comparison between the experimental and calculated UPS spectra ($\hbar\omega = 21.2$ eV) of clean annealed Si(111). Primaries and secondaries are shown by dashed and dotted lines. For clarity, the experimental curve has been shifted upwards to correspond to E_{VB} in Table VI.

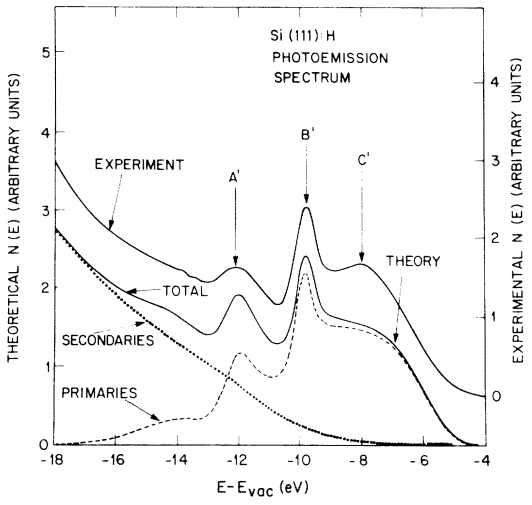

FIG. 6. Comparison between the experimental and calculated UPS spectra ($\hbar\omega = 21.2$ eV) of Si(111):H. Experimental curve has been shifted upwards to correspond to E_{VB} in Table VI.

which suggests that both A and the weak shoulder D are probably associated with superlattice (7×7) formation. The energies and overall intensities of features A–C agree almost perfectly.

In Fig. 6, a similar comparison is made for Si(111):H. The peak energies $E(A')$ and $E(B')$ agree very well. However, the experimental data contain a peak C' which is not present in the theoretical density of states, which contains only a plateau in the same energy region. The simplest of the explanations, that it is due to some foreign impurities (other than H), can be ruled out since during H deposition, the Auger spectrum of the sample surface was monitored continuously, and no impurities were detected. Similarly hydrogen molecules, which are most likely present, cannot be responsible for this peak since they do not adsorb at the surface. The most likely origin of this peak (C') is the superlattice structure of the surface (which is maintained on H chemisorption). Due to the reconstruction, there are at least some Si atoms in the surface unit cell which do not make normal Si–H bond and may give rise to the peak C'. However, due to good overall agreement with theoretical results (which is based on 1×1 structure) the number of such atoms must be small ($\lesssim 10\%$). Because of the vastly different oscillator strengths at the clean and hydrogenated surfaces, any effect due to reconstruction is likely to be much more pronounced in the UPS density of states of the latter. This is indeed the case as can be seen from Figs. 5 and 6. Another possible, though less likely explanation for C' may lie in our approximate treatment of the oscillator strengths which are assumed to be energy independent. For electrons near the valence-band maximum, the oscillator strengths show significant dependence on energy, photon polarization, and collector geometry.[31]

In Fig. 7, the photoemission spectra[2] of clean and H-chemisorbed Si(111) for $\hbar\omega = 16.8$ eV are compared with theoretical results. Theoretical spectra differ from the previous case ($\hbar\omega = 21.2$ eV) in two respects. First, the escape depth for the excited electron changes significantly ($L = 10$ Å in the present case as opposed to $L = 5$ Å for $\hbar\omega = 21.2$ eV). As a result, the primary electron distribution $N_p(E)$ is less surface sensitive. This can be easily seen from a reduction in the relative peak heights due to hydrogen. Second, due to lower photon energy, the secondary electron distribution function $N_s(E)$ decays much faster as the energy increases. As can be seen from Fig. 7, these two effects adequately account for the experimental data. In the present case, the agreement with experiment is not as good as for $\hbar\omega = 21.2$ eV, because our assumption of energy independent oscillator strength is better satisfied at higher photon energies.

The photoemission spectrum[3] of Ge(111):H for $\hbar\omega = 21.2$ eV is shown in Fig. 8 which also shows the theoretical result. Because of the similarity of the energy bands of Si and Ge, spectra for H

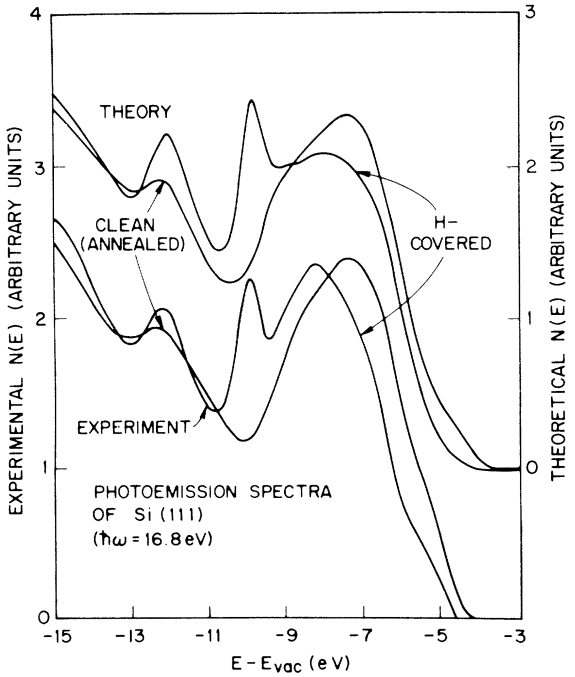

FIG. 7. Comparison between the experimental and calculated UPS spectra ($\hbar\omega = 16.8$ eV) of clean and H-covered Si(111).

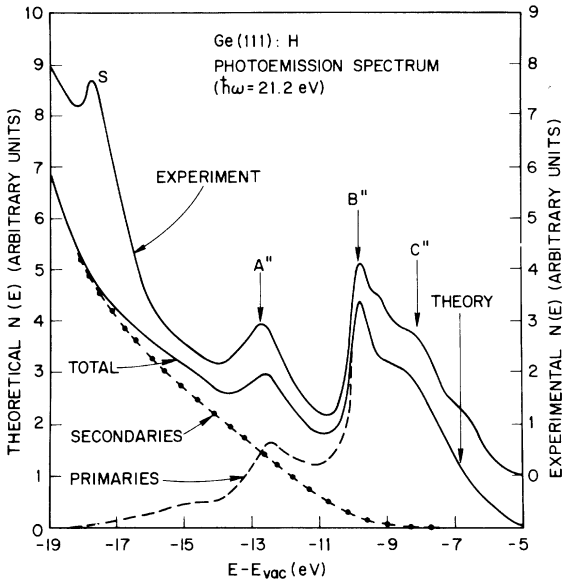

FIG. 8. Experimental UPS spectra ($\hbar\omega = 2.12$ eV) for Ge(111):H is compared with the theoretical calculation.

chemisorption on the two crystal surfaces are similar (e.g., A'', B'', and C'' correspond to the peaks A', B', and C' in Fig. 6).

VI. DISCUSSION

There have been a number of simple model calculations[34,35] for chemisorption on surfaces. The only realistic calculation, so far, is that due to Appelbaum and Hamann,[36] who carried out a self-consistent pseudopotential calculation for hydrogen chemisorption on Si(111). Because of the coarse sampling ($\Delta E \sim 1$ eV in their histogram) of the SBZ used by Appelbaum and Hamann in calculating the LDS at the hydrogen layer, detailed comparison of our spectrum ($\Delta E \sim 0.1$ eV) with that of the self-consistent calculation cannot be made. However, the LDS obtained from the two calculations are in good overall agreement. In the self-consistent calculation, the main peak (due to Si–H bond) in $\rho_1(E)$ lies at a higher energy (–4.8 eV) compared to the present TB calculation and experiment (both at –5.0 eV). Also, the amplitude of the peak at –10.0 eV in $\rho_1(E)$ is smaller in the self-consistent calculation.

One of the claims made by Appelbaum and Hamann is that the TB method fails to describe, even *qualitatively*, the energy bands of the chemisorbed surfaces.[36] This is in contradiction to the general belief that, because the H–Si bond is stronger (than Si–Si bond), the TB method should be well suited to this problem. Our present TB calculation, which we believe is the first *realistic* TB calculation for chemisorption, indeed shows that the conclusion reached by Appelbaum and Hamann is incorrect. Figures 5–8 clearly show that the results of the TB calculations are in *good quantitative* agreement with the UPS[1-3] data.

In the present TB model the Hamiltonian matrix elements (parameters) between the orbitals of the substrate and chemisorbed atoms are obtained from experimental data on molecular energy levels. Such a determination of the parameters is clearly not useful if the molecular energy levels are less sensitive to these parameters than are the surface states and resonances. In order to study this point and to obtain better insight into the chemisorption of hydrogen on Si, we have studied the surface energy bands and LDS for various sets of parameters. Since LDS are the quantities of greatest importance and can be measured experimentally, we will limit our discussion to them.

Figure 9 shows the variation of the LDS at the hydrogen atomic layer with E_H (the diagonal matrix element for hydrogen orbitals). The LDS corresponding to the parameters obtained from the molecular energy levels is shown by the curve in the middle ($\Delta E_H = 0.0$). This is the same as $\rho_1(E)$ in Fig. 3 and is reproduced here (center panel) for comparison. The curve at the top (bottom) panel is obtained by increasing (decreasing) E_H, by 1.0

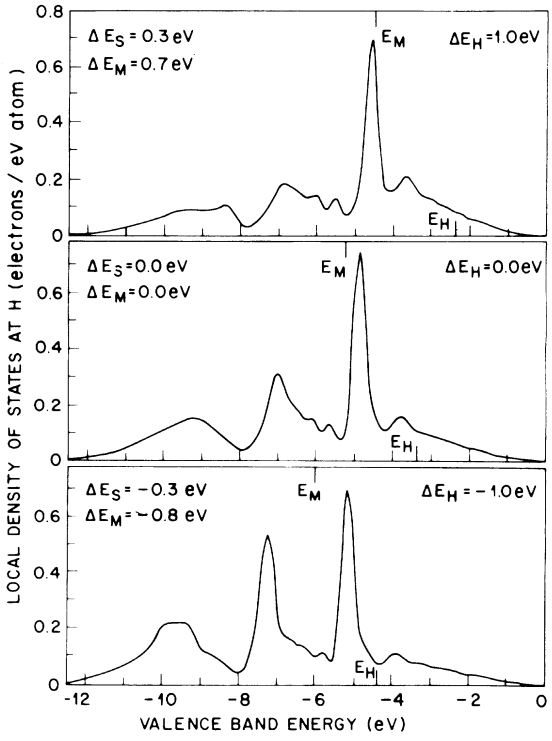

FIG. 9. E_H dependence of the hydrogen density of states, the surface state E_s and the molecular level E_M.

eV while keeping all other parameters fixed. Figure 10 shows the variation of the LDS at the hydrogen layer with the ($ss\sigma$) parameter (E_{ss}). The top panel curve is obtained by increasing E_{ss} by 1.0 eV while keeping E_H and the ratio $E_{ss}/E_{sp\sigma}$ fixed. The bottom curve is obtained similarly by decreasing E_{ss} by 1.0 eV.

Before going into detailed discussion of the variation of the LDS, it should be pointed out that the parameter changes (±1.0 eV) used to obtain Figs. 9 and 10 are very large (typically 30% of the parameter itself). Such a large variation is used in order to produce an appreciable change in the LDS. Any uncertainties in the parameter determined from molecular energy levels are likely to be an order of magnitude smaller (~0.3 eV) leading to a correspondingly small (unnoticeable) change in the LDS.

From Figs. 9 and 10, which also show the molecular energy level (E_M) of SiH_4 ($s_H p_{Si}\sigma$ bonding state of t_2 symmetry), we notice that the main peak (E_s) in LDS (at about −5.0 eV) is relatively insensitive to the variations in E_H. As expected, both E_s and E_M move to higher (lower) energy for increasing (decreasing) E_H. Similar behavior is observed with changes in ($ss\sigma$) parameter, (denoted by E_{ss} in Fig. 10) where because of a stronger (more attractive) interaction the energy of the bonding states (E_s and E_M) is lowered. The peak intensities, however, change appreciably with the parameters. For lower hydrogen orbital energy or a stronger Si–H interaction, there is stronger hybridization of the hydrogen 1s orbital with the lower-lying Si states (s type), thus increasing the intensity of the corresponding peaks. In both cases additional surface states appear below the bottom of the valence band and in the gap region near −7.5 eV (Fig. 2). Both the surface state (E_s) and molecular level (E_M) move to higher energy with increasing E_H (Fig. 9). As a result of weaker hybridization of the hydrogen 1s orbital with the low-lying s states of Si, the low-energy peaks in the LDS are considerably reduced (Fig. 9). For ΔE_{ss} = 1.0 eV, (Fig. 10), the coupling between the hydrogen and Si orbitals is very weak and the hydrogen density of states is dominated by a single peak (atomic type of behavior).

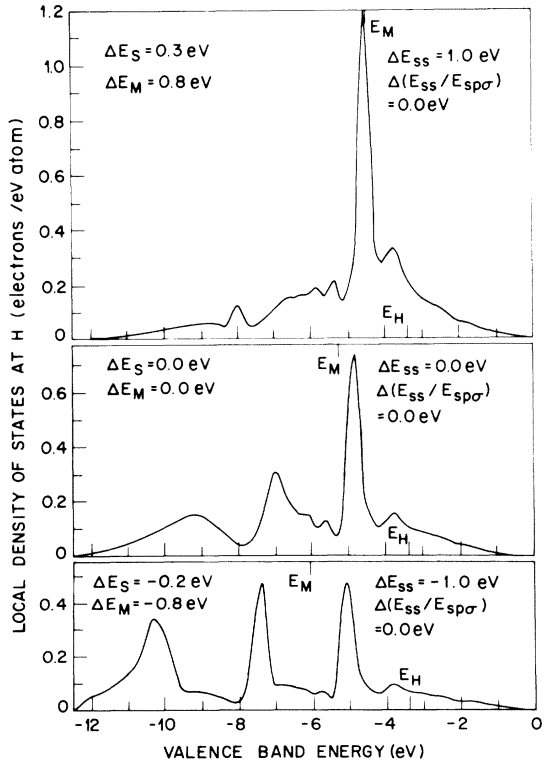

FIG. 10. Variation of the hydrogen density of states, the surface state E_s and the molecular level E_M with E_{ss} (see text).

Figures 9 and 10 show that both E_s and E_M vary linearly with E_H and E_{ss} over a relatively large region and that the molecular levels are about three times as sensitive as the surface states to the variation of parameters (i.e., $\Delta E_M/\Delta E_s \sim 3$). The relative insensitivity of the surface states is due to two main reasons. First, at the surface only one of the bonds H–Si (Ge) is altered as opposed to SiH_4 (GeH_4), where all four are altered. Second, the existence of a surface state is determined to a large degree by the surface geometry and the bulk energy bands which determine the forbidden energy regions (for a given $\vec{k}_{\parallel}$) in which the surface states are pinned.

In the TB approximation, surface states and resonances are most easily obtained by calculating the electronic states of a slab of finite thickness.[10-13] If the slab is sufficiently thick, its electronic states will be identical to that of semi-infinite solid (except for the two-fold degeneracy arising from the two identical surfaces in the slab). However, the computation time increases with the cube of the slab thickness, so for reasons of economy one uses the slab of minimum thickness that still represents the semi-infinite solid with sufficient accuracy. The main criterion for the determination of the slab thickness is that its properties should be independent of the thickness beyond the minimum value. For clean Si and Ge surfaces it was shown[10-13] that a slab consisting of about 20 atomic layers is a good approximation to the semi-infinite solid. For such a slab the splitting between the surface states on the two sides is ~0.01 eV and the LDS on the central layer is the same (to within about 3%) as the bulk density of states.

In Fig. 11 we show the LDS at the hydrogen atomic layer for three different slabs of thickness 18, 22, and 30 atomic layers. In all three cases, the splitting of the surface states (at -5 eV) on the two surfaces is very small ($\lesssim 0.01$ eV). However, there is significant dependence of the LDS on thickness (Fig. 11). Similar dependence is observed for the LDS on other layers as well. The most significant effect of increasing the thickness from 18 to 22 to 30 layers is that the sharp peaks in the region $-7 < E < -5$ eV gradually disappear. The origin of these peaks (in the 18-layer calculation) can be easily understood by looking at the bulk energy bands of Si (Fig. 1). Near the zone center of the surface Brillouin zone, the surface states and resonances are derived from the bulk states along the Λ line ($\Gamma - L$) in Fig. 1. In a slab of finite thickness, only a discrete set of states along Λ contribute to the surface resonances (which are absent from clean surfaces because of relatively weak interaction) giving rise to peaks in the LDS. These peaks are well separated in energy due to large bandwidth (Fig. 1) of the bulk band along Λ (Fig. 1). These peaks are continuously distributed for infinitely thick slab, giving a smooth LDS in this region. While the small peak at -5.5 eV in the hydrogen LDS for 30 layers may still be due to finite thickness, from the relatively small change in LDS in going from 22 to 30 layers we judge that the latter case is a very good approximation to semi-infinite solids. The above discussion shows that the minimum slab thickness required, in general, depends on the problem under study and slabs of varying thickness should be used to eliminate any errors. We also notice that the results obtained from the calculations on small clusters can not be applied to clean ordered surfaces.

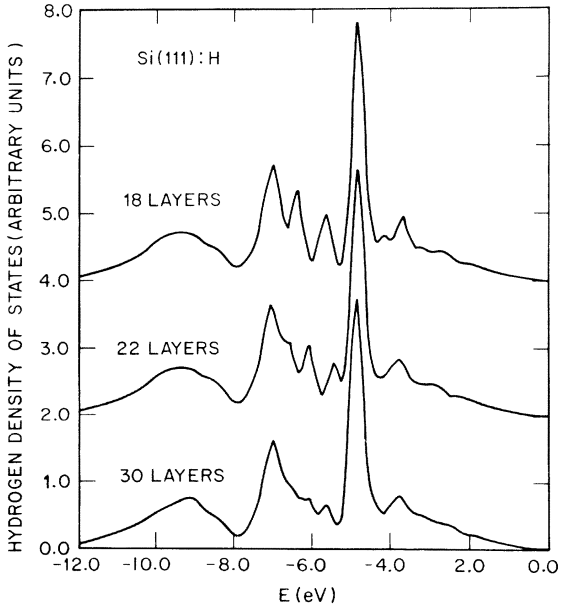

FIG. 11. Dependence of the hydrogen density of states on slab thickness.

ACKNOWLEDGMENTS

We are very grateful to J. C. Phillips for several valuable discussions and comments on the manuscript. Thanks are due to H. D. Hagstrum, J. E. Rowe, and T. Sakurai for providing us with experimental UPS data prior to publication.

APPENDIX A

In this appendix the molecular orbital energies and wave functions of tetrahedral molecules SiH_4 and GeH_4 are discussed.

Because of the tetrahedral symmetry of the molecule, the 8×8 Hamiltonian matrix can be block-diagonalized into four 2×2 matrices. One of these matrices corresponds to the level of s symmetry (about Si or Ge atom) and gives rise to $a_1^{\pm}$ levels (bonding and antibonding). The other three matrices give rise to the triply degenerate p-type states ($t_2^{\pm}$ bonding and antibonding).

Using the symmetrized combination of atomic orbitals of a_1 and t_2 symmetry and solving the 2×2 matrix it can be easily shown that the molecular energy levels are given by

$$E_{a_1}^{\pm} = \tfrac{1}{2}(E_H + 3\gamma + E_s) \pm [\tfrac{1}{2}(E_H + 3\gamma + E_s)^2 + 4\alpha^2]^{1/2} \tag{A1}$$

and

$$E_{t_2}^{\pm} = \tfrac{1}{2}(E_H - \gamma + E_p) \pm [\tfrac{1}{2}(E_H - \gamma - E_p)^2 + \tfrac{4}{3}\beta^2]^{1/2}, \tag{A2}$$

where E_H, E_s, and E_p refer to the atomic energy levels of hydrogen and the s and p orbital energies of Si or Ge. The constants α and β are respectively the $(ss\sigma)$ and $(sp\sigma)$ interaction parameters of hydrogen and Si (or Ge). The second-neighbor hydrogen-hydrogen $(ss\sigma)$ interaction is denoted by γ. The calculated energy levels, using the parameters listed in Tables I and III, are given in Table II.

The corresponding wave functions are given by

$$\Psi_{a_1}^{\pm} = \varphi_s + [(E_{a_1}^{\pm} - E_s)/4\alpha](\varphi_1 + \varphi_2 + \varphi_3 + \varphi_4) \tag{A3}$$

and

$$\Psi_{t_2}^{\pm} = \varphi_{p_x} + \sqrt{3}\,[(E_{t_2}^{\pm} - E_p)/4\beta](\varphi_1 + \varphi_2 - \varphi_3 - \varphi_4), \tag{A4}$$

where the hydrogen orbitals located at (111),

$(1\bar{1}\bar{1})$, $(\bar{1}\bar{1}1)$, and $(\bar{1}1\bar{1})$ corners of the tetrahedron are denoted by φ_i $(i=1,4)$ and φ_s and φ_p are the s and p orbitals of Si.

APPENDIX B

In this appendix we discuss briefly the spectrum of the secondary electrons created in photoemission.

The secondary electrons are created by electron hole pair production by a high energy primary electron. Kane[29] has studied pair production in Si and has shown that the distribution function for secondary electrons of energy E^s produced by a primary electron of energy E^p is given by

$$S(E^p,E^s)=2\rho(E^s)\int\rho(E')\rho(E'')\,dE' \times\left(\int\rho(E^s)\rho(E')\rho(E'')\,dE^s\,dE'\right)^{-1}, \tag{B1}$$

where energy conservation requires that

$$E^p=E^s+E'-E''. \tag{B2}$$

E' and E'' are respectively the final-state electron and hole energies so that

$$E^s,E^p,E'\geq E_F;\quad E''\leq E_F, \tag{B3}$$

and ρ denotes the density of states. Equation (B1) is based on "random-$\vec{k}$ approximation" (momentum conservation has been ignored) whose validity has been demonstrated by Kane.[29]

Assuming a constant matrix element for optical excitation (energy and $\vec{k}$ independent) and a constant escape probability, the secondary electron distribution due to all photoexcited electrons is given by

$$S_T(E^s)\propto\int\rho(E_v)\rho(E_v+\hbar\omega)S(E_v+\hbar\omega,E^s)dE_v, \tag{B4}$$

where $\hbar\omega$ is the photon energy and E_v is the valence band energy. It should be noted that in (B4) the secondary electron distribution depends only on the density of states of the valence and conduction bands. In the tight-binding approximation while the valence bands are accurately given, the conduction bands contain substantial errors. As a result, in the secondary electron distribution functions we have used Kane's conduction band density of states based on the pseudopotential method.[37]

*Present address: IBM Thomas J. Watson Research Center, Yorktown Heights, NY 10598.

[1]H. Ibach and J. E. Rowe, Surf. Sci. 43, 481 (1974).
[2]T. Sakurai and H. D. Hagstrum, Phys. Rev. B 12, 5349 (1975).
[3]J. E. Rowe, Solid State Commun. 17, 673 (1975).
[4]D. E. Eastman and W. D. Grobman, Phys. Rev. Lett. 28, 1378 (1972).
[5]L. F. Wagner and W. E. Spicer, Phys. Rev. Lett. 28, 1381 (1972).
[6]J. E. Rowe and H. Ibach, Phys. Rev. Lett. 31, 102 (1973).
[7]J. E. Rowe and H. Ibach, Phys. Rev. Lett. 32, 421 (1974).
[8]J. E. Rowe, M. M. Traum, and N. V. Smith, Phys. Rev. Lett. 33, 1333 (1974).
[9]J. A. Appelbaum and D. R. Hamann, Phys. Rev. Lett. 31, 106 (1973).
[10]K. C. Pandey and J. C. Phillips, Solid State Commun. 14, 439 (1974).
[11]K. C. Pandey and J. C. Phillips, Phys. Rev. Lett. 32, 1433 (1974).
[12]K. C. Pandey and J. C. Phillips, Phys. Rev. Lett. 34, 1450 (1975).
[13]K. C. Pandey and J. C. Phillips, Phys. Rev. B 13, 750 (1976).
[14]H. D. Hagstrum and G. E. Becker, Phys. Rev. B 8, 1580; 1592 (1973).
[15]M. L. Cohen and T. K. Bergestresser, Phys. Rev. 141, 789 (1966).
[16]K. C. Pandey and J. C. Phillips, Phys. Rev. B 9, 1552 (1974).
[17]G. Dresselhaus and M. S. Dresselhaus, Phys. Rev. 160, 649 (1967).
[18]G. E. Becker and G. W. Gobeli, J. Chem. Phys. 38, 2942 (1963).
[19]R. G. Cavell, S. P. Kowalczyk, L. Ley, R. A. Pollack, B. Mills, D. A. Shirley, and W. Perry, Phys. Rev. B 7, 5313 (1973).
[20]M. L. Sink and G. E. Juras, Chem. Phys. Lett. 20, 474 (1973).
[21]A. W. Potts and W. C. Price, Proc. R. Soc. A 326, 165 (1972); W. C. Price and G. R. Wilkinson (unpublished).
[22]R. Hoffman, J. Chem. Phys. 39, 1397 (1963).
[23]D. P. Santry and G. A. Segal, J. Chem. Phys. 47, 158 (1966).
[24]R. S. Mulliken, J. Chem. Phys. 46, 497, 675 (1949).
[25]L. Pauling, *The Nature of Chemical Bond* (Cornell U. P., Ithaca, N. Y., 1960), p. 64.
[26]K. Siegbahn, *ESCA Applied to Free Molecules* (North-Holland, Amsterdam, 1969), p. 104.
[27]J. W. Gadzuk, Surf. Sci. 43, 44 (1974); M. J. Kelly, *ibid.* 43, 587 (1974).
[28]F. Cyrot-Lackmann, Adv. Phys. 16, 393 (1967); J. Phys. Chem. Solids 29, 1235 (1968).
[29]E. O. Kane, Phys. Rev. 159, 624 (1967).
[30]W. D. Grobman, D. E. Eastman, J. L. Freeouf, and J. Shaw, in *Proceedings of the Twelfth International Conference on the Physics of Semiconductors* (Teubner, Stuttgart, 1974), p. 1275.
[31]J. P. Van Dyke, Phys. Rev. B 5, 4206 (1972).
[32]K. C. Pandey and J. C. Phillips, Solid State Commun.

(to be published).
[33]J. E. Rowe, Phys. Rev. Lett. 34, 398 (1975).
[34]S. G. Davisson and J. D. Levine, in *Solid State Physics*, edited by H. Ehrenreich, F. Seitz, and D. Turnbull (Academic, New York, 1970), Vol. 25.
[35]T. L. Einstein and J. R. Schrieffer, Phys. Rev. B 7, 3629 (1973).
[36]J. A. Appelbaum and D. R. Hamann, Phys. Rev. Lett. 34, 806 (1975).
[37]E. O. Kane, Phys. Rev. 146, 558 (1966).

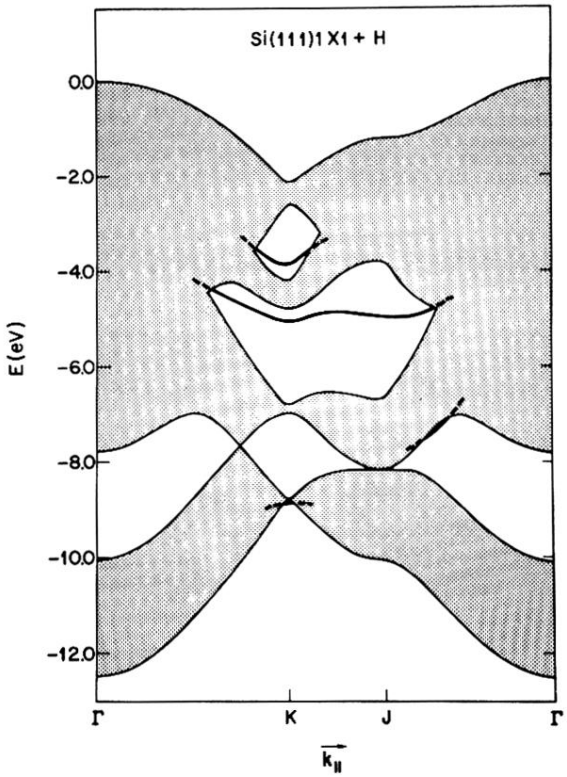

FIG. 2. Surface energy bands for hydrogen chemisorbed on Si(111)1×1. For a fixed surface wave vector $\vec{k}_{\parallel}$ true surface states (shown by heavy lines) exist only in the energy gap of the bulk bands obtained by varying $\vec{k}_{\perp}$. The region where no such gap exists is shown by the dotted area. The center of the surface Brillouin zone (a hexagon) is denoted by Γ. The edge center and corner are denoted by J and K respectively.